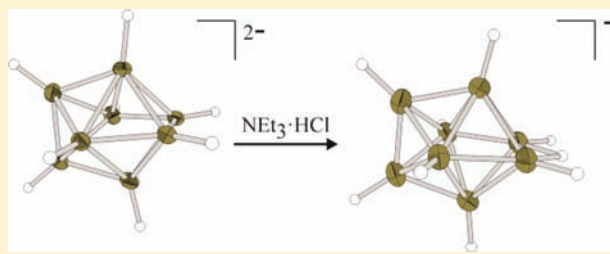# Syntheses and Crystal Structures of the *closo*-Borate M[B_8H_9] (M = [PPh$_4$]$^+$ and [N(*n*-Bu$_4$)]$^+$)

Florian Schlüter and Eduard Bernhardt*

Fachbereich C—Anorganische Chemie, Bergische Universität Wuppertal, Gaußstraße 20, 42119 Wuppertal, Germany
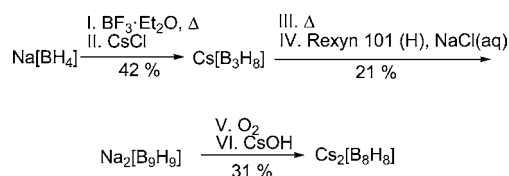
S *Supporting Information*

ABSTRACT: Protonation of $M_2[B_8H_8]$ with HCl or $NEt_3 \cdot HCl$ resulted in $M[B_8H_9]$ (M = $[PPh_4]^+$ or $[N(n\text{-}Bu_4)]^+$). The monoanion was isolated and characterized by ^1H, $^1H\{^{11}B\}$, ^{11}B, and $^{11}B\{^1H\}$ NMR spectroscopy. The "protonated" form $[B_8H_9]^-$ showed a dynamic behavior in solution, which was analyzed by NMR spectroscopy and compared with theoretical calculations. The structures of $[B_8H_9]^-$ as well as $[B_8H_8]^{2-}$ were determined by single-crystal X-ray diffraction.

■ INTRODUCTION

In contrast to the *closo*-borate dianions $[B_nH_n]^{2-}$ ($n = 6{-}12$), which were synthesized between 1959 and 1967,[1-5] the corresponding protonated borates $[B_nH_{n+1}]^-$ ($n = 6{-}12$) have only been rarely investigated. While the crystal structures of the *closo*-borates $[B_nH_n]^{2-}$ ($n = 6{-}12$) were determined, only those of $[B_6H_7]^-$,[6-9] $[B_7H_8]^-$,[10] and $[B_{10}H_{11}]^{-11}$ were published; for an overview of the crystal structures of $[B_nH_n]^{2-}$ ($n = 6{-}12$), see ref 10 and reference therein. The syntheses of the protonated forms $[B_nH_{n+1}]^-$ ($n = 6, 7, 10$) were carried out in different ways. The monoanion $[B_6H_7]^-$ is available from $[N(n\text{-}Bu_4)]_2[B_6H_6]$ by protonation with hydrochloric acid.[12] Protonation of $[B_7H_7]^{2-}$ with $NEt_3 \cdot HCl$ leads to the anion $[B_7H_8]^-$. A protonation of $[N(n\text{-}Bu_4)]_2[B_7H_7]$ with hydrochloric acid is possible as well. Small amounts of $[N(n\text{-}Bu_4)][B_6H_7]$ were observed in this case.[10] The strong trifluoroacetic acid is necessary to synthesize $[B_{10}H_{11}]^-$, starting from $[B_{10}H_{10}]^{2-}$.[11,13,14]

Scheme 1. Synthesis of $[B_8H_8]^{2-}$, Starting from Na[BH$_4$]^a

Na[BH$_4$] $\xrightarrow[\text{42 \%}]{\substack{\text{I. BF}_3\cdot\text{Et}_2\text{O, }\Delta \\ \text{II. CsCl}}}$ Cs[B$_3$H$_8$] $\xrightarrow[\text{21 \%}]{\substack{\text{III. }\Delta \\ \text{IV. Rexyn 101 (H), NaCl(aq)}}}$ Na$_2$[B$_9$H$_9$] $\xrightarrow[\text{31 \%}]{\substack{\text{V. O}_2 \\ \text{VI. CsOH}}}$ Cs$_2$[B$_8$H$_8$]

^{a}Literature: steps I and II, ref 15; steps III and IV, ref 4; and steps V and VI, ref 3.

In Scheme 1 the synthesis of $[B_8H_8]^{2-}$, which was reported in 1967,[3] is shown. The dianion is available in 6 steps starting from sodium boron hydride; the overall yield is 3%.

A synthesis of the monoanion $[B_8H_9]^-$ has not been published so far. For the labeling of $[B_8H_9]^-$, see Figure 1
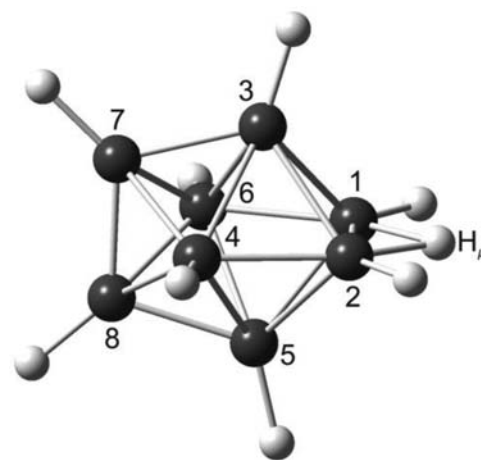

Figure 1. Labeling of the positions in $[B_8H_9]^-$.

The syntheses of smaller borates such as $[B_8H_9]^-$ are of general interest. The reasons are their unique bonding situations and the fact that simple *closo*-borates are valuable starting materials for further borate anions.[16]

Up to now there have been some theoretical and experimental studies about the dynamic NMR behavior of $[B_8H_8]^{2-}$ and $[B_8H_9]^-$; available examples are given in refs 17–21 and references therein. Two different signal sets for $[B_8H_8]^{2-}$ were generally observed in the NMR spectra: In a mixture of CH_2Cl_2/toluene, three signals with an intensity of 2:4:2 ($\delta = -22.2, -3.6,$ and 9.5 ppm) for $[N(n\text{-}Bu_4)]_2[B_8H_8]$ were found, while in water one signal ($\delta = -6.8$ ppm) for $Cs_2[B_8H_8]$ was detected.[19-21] In the case of $Na_2[B_8H_8]\cdot xH_2O$ in 1,2-dimethoxyethane both signal sets (the single and 2:4:2 set) were observed at the same time.[19] Those results were

interpreted in terms of three polytopal isomeric forms which may interconvert (Figure 2).[19−21]

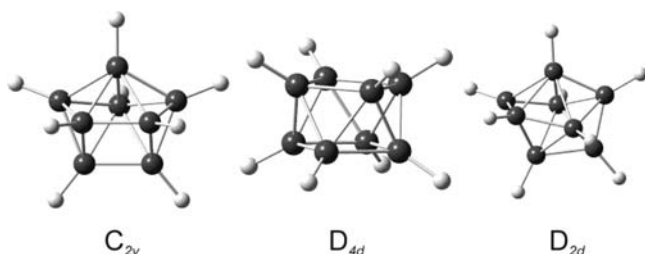**Figure 2.** Polytopal isomeric forms of $[B_8H_8]^{2-}$.

The C_{2v}-bicapped trigonal prismatic form can explain the three doublets with an intensity of 2:4:2. The single doublet was assigned to the D_{4d} square antiprismatic form.[20] The fluxional D_{2d} form, which also could account for the single signal, was excluded, as the boron scrambling mechanism should proceed via the D_{4d} intermediate. This was supposed to be in a fast equilibrium with the C_{2v} isomer. Hence, the fluxional D_{2d} form and the static C_{2v} form should not coexist.[17,20] In a theoretical paper[18] Kleier and Libscomb presented that the dynamic behavior of $[B_8H_8]^{2-}$ could not be based on the stable D_{4d} form, as this form is too high in energy. D_{2d}, however, was computed to be the most stable isomer.[17,18] The calculations were refined in 1992 at modern computational levels, and it was found that the most stable $[B_8H_9]^-$ structure showed C_{2v} symmetry and the 2:4:2 signal set was assigned to $[B_8H_9]^-$.[17]

We report here on a synthesis for $M[B_8H_9]$ ($M = [PPh_4]^+$ (tetraphenylphosphonium) and $[N(n\text{-}Bu_4)]^+$ (tetrabutylammonium). The anion was characterized by ^1H, $^1H\{^{11}B\}$, ^{11}B, $^{11}B\{^1H\}$ NMR spectroscopy and X-ray crystallography. In addition, the dynamic NMR behavior, which has not been fully understood until now, will be discussed.

■ EXPERIMENTAL SECTION

Chemicals. All chemicals were obtained from commercial sources. Solvents were dried and stored in flasks equipped with valves with PTFE stems (Young, London) over molecular sieves (4 Å) under an argon atmosphere. $Cs[B_3H_8]$,[15] $Cs_2[B_8H_8]$,[3] and $Cs_2[B_9H_9]$[4] were prepared according to known procedures.

Synthesis. *$[N(n\text{-}Bu_4)][B_8H_9]$.* $Cs_2[B_8H_8]$[3] (1.80 g, 5.00 mmol) was dissolved in 650 mL of H_2O. $[N(n\text{-}Bu_4)]Br$ (4.84 g, 15.00 mmol) in 100 mL of H_2O was added under stirring and 10 mL of concentrated HCl was added. The resulting colorless precipitate was separated, washed with H_2O (50 mL), and dried in vacuum. Yield: 1.69 g, 5.00 mmol, 100%.

$^1H\{^{11}B\}$ NMR (400 MHz, CD_2Cl_2, 27 °C): δ = 1.06 (t, 12 H, CH_3, $^3J_{HH}$ = 7.2), 1.47 (m, 8 H, CH_2CH_3), 1.65 (m, 8 H, $CH_2CH_2CH_3$), 3.14 (m, 8 H, NCH_2), 3.9 (s, very broad), H, $[B_8H_9]^{2-}$). $^{11}B\{^1H\}$ NMR (128 MHz, CD_2Cl_2, 27 °C): δ = 9.4 (s, 2 B, B7, B8), −3.5 (s, 4 B, B1 B2, B4, B6), −21.6 (s, 2 B, B3, B5).

$[PPh_4]_2[B_8H_8]$. $Cs_2[B_8H_8]$[3] (0.20 g, 0.55 mmol) was dissolved in 180 mL of 1 M NaOH solution at 60 °C, and $[PPh_4]Cl$ (0.44 g, 1.13 mmol) in 60 mL of H_2O was added. The red residue was separated after stirring for 15 min, washed with H_2O (60 mL), and dried in vacuum. Yield: 0.42 g (100%).

$^1H\{^{11}B\}$ NMR (400 MHz, CD_2Cl_2, 27 °C): δ = 7.98−7.66 (m, 40 H, 2$[PPh_4]^+$), 2.25 (s, 8 H, $[B_8H_8]^{2-}$). ^{11}B NMR (128 MHz, CD_2Cl_2, 27 °C): δ = −5.0 (d, 8 B, $[B_8H_8]^{2-}$). ^{31}P NMR (162 MHz, CD_2Cl_2, 27 °C): δ = 23.1 (s, 2 P, 2$[PPh_4]^+$).

$[PPh_4][B_8H_9]$. This compound was prepared under argon atmosphere, using Schlenk line techniques and dry solvents. $[PPh_4]_2[B_8H_8]$

(0.42 g, 0.54 mmol) and $NEt_3\cdot HCl$ (0.15 g, 1.08 mmol) were placed in a flask under an argon atmosphere, and 15 mL of dry CH_3CN was added under stirring. The solution was stirred for 15 min, and then 100 mL of dry diethyl ether was added carefully with a syringe to the solution. Colorless crystals, which were formed after 5 days, were dried in vacuum overnight. A 50 mL portion of H_2O was added, and the suspension was stirred for 15 min. The solid was separated, washed again with 25 mL of H_2O, and dried in vacuum. Yield: 0.23 g (100%).

$^1H\{^{11}B\}$ NMR (400 MHz, CD_2Cl_2, 27 °C): δ = 7.98−7.63 (m, 20 H, $[PPh_4]^+$), 3.8 (s, (very broad) H, $[B_8H_9]^-$). $^{11}B\{^1H\}$ NMR (128 MHz, CD_2Cl_2, 27 °C): δ = 8.7 (s, 2 B, B7, B8), −4.0 (s, 4 B, B1, B2, B4, B6), −21.4 (s, 2 B, B3, B5). ^{31}P NMR (162 MHz, CD_2Cl_2, 27 °C): δ = 23.1 (s, 1 P, $[PPh_4]^+$).

Hydrogen−deuterium exchange in $[PPh_4]_2[B_8H_8]$ (*in situ*): $[PPh_4]_2[B_8H_8]$ (0.07 g, 0.08 mmol) was dissolved in CH_2Cl_2/NPr_3 (15 mL/2 mL), and a 0.1 M NaOH solution (15 mL) was added. $Na[BPh_4]$, in 0.1 M NaOH (15 mL) was added, and after filtration over Celite, the aqueous layer was separated. K_2CO_3 (0.023 g in 5 mL of H_2O) was added, and after filtration of $K[BPh_4]$ over Celite, the aqueous solution was evaporated to dryness. In D_2O, under basic conditions, no substitution of H and D was observed. After neutralization with CO_2 ($\approx$pH 7), a substitution of all eight H atoms by D atoms was observed after a few hours, as evident from the ^{11}B NMR spectrum.

Crystal Structure Determination. Crystals were centered on an Oxford Diffraction Gemini E Ultra diffractometer, equipped with a 2K×2K EOS CCD area detector, a four-circle κ goniometer, an Oxford Instruments Cryojet, and sealed-tube Enhanced (Mo) and Enhanced Ultra (Cu) sources. For data collection, the Cu source emitting monochromated Cu $K\alpha$ radiation (λ = 1.54184 Å) or Mo $K\alpha$ radiation (λ = 0.71073 Å) was used. The diffractometer was controlled with the CrysAlisPro Graphical User Interface (GUI) software.[22] Processing of the raw data, scaling of diffraction data, and the application of an empirical absorption correction was completed by using the CrysAlisPro program.[34]

Crystallographic data for $Cs_2[B_8H_8]$ (**1**, CCDC 838035), $[PPh_4]_2[B_8H_8]\cdot CH_2Cl_2$ (**2, 3**, CCDC 838036 and 838037), $[Ph_4P]$-$[B_8H_9]$ (**4, 5, 6**, CCDC 838038, 838039, and 838040), and $[N(n\text{-}Bu_4)][B_8H_9]$ (**7**, CCDC 838041) were deposited with the Cambridge Crystallographic Data Centre, 12 Union Road, Cambridge CB21EZ, U.K. Copies of the data can be obtained at www.ccdc.cam.ac.uk/data_request/cif; fax, +44-1223-336-033; e-mail, deposit@ccdc.cam.ac.uk.
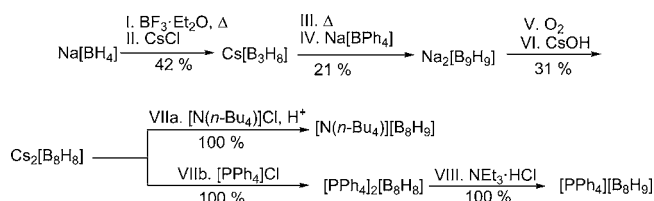
NMR. A Bruker ARX 400 (400.13 MHz for ^1H, 128.38 MHz for ^{11}B, and 161.97 MHz for ^{31}P) and dichloromethane-d_2 as solvent were used. External standards are $SiMe_4$ ($\delta(^1H)$ = 0 ppm), $BF_3\cdot OEt_2$ ($\delta(^{11}B)$ = 0 ppm), and 85% H_3PO_4 ($\delta(^{31}P)$ = 0 ppm).

Theoretical Calculations. Quantum chemical calculations were performed to support the experimental results. DFT calculations[23] were carried out with the B3LYP-Method.[24−26] The 6-311++G(d,p) basis set was used as implemented in the Gaussian03 program suite.[27] The shielding constants (GIAO)[28−32] and the coupling constants were calculated as described in the literature.[33−36] Intrinsic reaction path (IRC) calculations were performed for all transition states.[37,38]

■ RESULTS AND DISCUSSION

Synthesis. The synthesis of the $[B_8H_8]^{2-}$ anion was first published in 1967.[3] The oxidation of $Na_2[B_9H_9]$ with oxygen in dimethoxyethane leads to the $[B_8H_8]^{2-}$ dianion as the main product, as depicted in Scheme 2.

Adding a solution of $[PPh_4]Cl$ in water to an aqueous solution of $Cs_2[B_8H_8]$ results in a deep red colored solid, $[PPh_4]_2[B_8H_8]$. The monoanion $[PPh_4][B_8H_9]$ is easily prepared from the dianion with $NEt_3\cdot HCl$ in quantitative yield. The deep red color vanishes immediately after addition of $NEt_3\cdot HCl$ in CH_3CN to a solution of the dianion in CH_3CN. Removing all volatile material and washing with water gives the colorless solid $[PPh_4][B_8H_9]$.

Scheme 2. Synthesis of $[B_8H_8]^{2-}$, Starting from $Na[BH_4]^a$

$$Na[BH_4] \xrightarrow[\substack{\text{I. } BF_3 \cdot Et_2O, \Delta \\ \text{II. } CsCl \\ 42\%}]{} Cs[B_3H_8] \xrightarrow[\substack{\text{III. } \Delta \\ \text{IV. } Na[BPh_4] \\ 21\%}]{} Na_2[B_9H_9] \xrightarrow[\substack{\text{V. } O_2 \\ \text{VI. } CsOH \\ 31\%}]{}$$

$$Cs_2[B_8H_8] \xrightarrow{\quad} \begin{cases} \xrightarrow[\substack{\text{VIIa. } [N(n\text{-}Bu_4)]Cl, H^+ \\ 100\%}]{} [N(n\text{-}Bu_4)][B_8H_9] \\ \xrightarrow[\substack{\text{VIIb. } [PPh_4]Cl \\ 100\%}]{} [PPh_4]_2[B_8H_8] \xrightarrow[\substack{\text{VIII. } NEt_3 \cdot HCl \\ 100\%}]{} [PPh_4][B_8H_9] \end{cases}$$

^{a}Literature: steps I and II, ref 15; step III, ref 4; step IV, this work; steps V and VI, ref 3; steps VII and VIII, this work.

Dissolving $Cs_2[B_8H_8]$ and $[N(n\text{-}Bu)_4]Br$ in water and acidification with HCl results in $[N(n\text{-}Bu_4)][B_8H_9]$ as a colorless solid, in quantitative yield. $[N(n\text{-}Bu_4)]_2[B_nH_n]$ ($n = 6–8$) are soluble in water and stable under basic conditions, whereas $[N(n\text{-}Bu_4)]_2[B_nH_n]$ ($n = 9–12$) are insoluble. In the case of $[PPh_4]_2[B_nH_n]$, only the salts with $n = 6$ and 7 are soluble in water. The other salts precipitate by adding $[PPh_4]Cl$ to an aqueous solution of $[B_nH_n]^{2-}$ ($n = 8–12$). The protonated forms show a deviant behavior: $[N(n\text{-}Bu_4)]$-$[B_nH_{n+1}]$ ($n = 6–8$) are not soluble in an aqueous solution. Protonation of $[N(n\text{-}Bu_4)]_2[B_8H_8]$ with aqueous HCl yields $[N(n\text{-}Bu_4)][B_8H_9]$, as mentioned before. Protonation of $[N(n\text{-}Bu_4)]_2[B_7H_7]$ under the same conditions leads to a mixture of $[N(n\text{-}Bu_4)][B_6H_7]$ and $[N(n\text{-}Bu_4)][B_7H_8]$. Hence, the protonation of $[N(n\text{-}Bu_4)]_2[B_7H_7]$ succeeds with $NEt_3 \cdot HCl$,[10] as described for $[B_8H_9]^-$, starting from $[PPh_4]_2[B_8H_8]$.

NMR Spectroscopy. Of the basic *closo*-borates $[B_nH_n]^{2-}$ ($n = 6–12$), only $[B_8H_8]^{2-}$ (refs 3, 18, 19, and 39) and $[B_{11}H_{11}]^{2-}$ (refs 4 and 40) show a dynamic behavior at ambient temperatures in solution.[17] The X-ray structure of $[B_8H_8]^{2-}$ shows a dodecahedron with D_{2d} geometry (see ref 39 and this work). It can be concluded that there are two sets of nonequivalent boron atoms. In the ^{11}B NMR spectra of $[PPh_4]^+$ or $[N(n\text{-}Bu_4)]^+$ salts in CD_2Cl_2 only one signal at -5.0 ppm can be obseverd. $Cs_2[B_8H_8]$ gives in D_2O one signal at -6.4 ppm.

As mentioned before, the most stable structure of $[B_8H_9]^-$ shows C_{2v} symmetry.[17] The extra proton is localized above the B1B2 edge, as shown in Figure 1. Four signals with an intensity of 2:2:2:2 are expected for this anion. The chemical shifts are very similar for B1,B2 (-0.9 ppm) and B4,B6 (-1.5 ppm).[17] The spectrum might appear to consist of only three peaks with an intensity of 2:4:2,[17] which were observed previously by experimental studies, but the signals were then assigned to the C_{2v} form of $[B_8H_8]^{2-}$.[19–21]

We found that the protonated form $[B_8H_9]^-$, which is now experimental available, gives three signals with an intensity of 2:4:2. The ^{11}B-NMR spectra at various temperatures for $[N(n\text{-}Bu_4)][B_8H_9]$ and $[N(n\text{-}Bu_4)]_2[B_8H_8]$ are given in Figure 3.

The dianion shows, as expected for the dynamic *closo*-borate, only one doublet. The chemical shifts of $[B_8H_9]^-$ (B7/B8 = 9.4, B1/B2/B4/B6 = -3.5, and B3/B5 = -21.6 ppm) are in agreement with the calculated ones.[17] Cooling down to -50 °C shows a change in the ^{11}B NMR spectrum. No coupling of boron to proton was detected at room temperature. At -50 °C, however, a coupling was observed (B7/B8: δ 9.5 ppm; $^1J(^{11}B, ^1H) = 156$ Hz; B1/B2/B4/B6: δ -3.7 ppm; $^1J(^{11}B, ^1H) = 137$ Hz; and B3/B5: δ -22.0 ppm; $^1J(^{11}B, ^1H) = 134$ Hz) (see also Supporting Information).

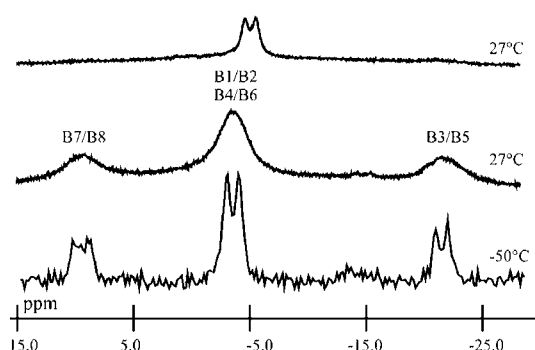In contrast to the ^{11}B NMR spectrum, the ^1H NMR spectrum shows a highly dynamic behavior. At room temper-

Figure 3. ^{11}B NMR spectra of $[N(n\text{-}Bu_4)][B_8H_9]$ at room temperature (center) and at -50 °C (bottom) and ^{11}B spectrum of $[N(n\text{-}Bu_4)_2][B_8H_8]$ at room temperature (top); measurements in CD_2Cl_2.
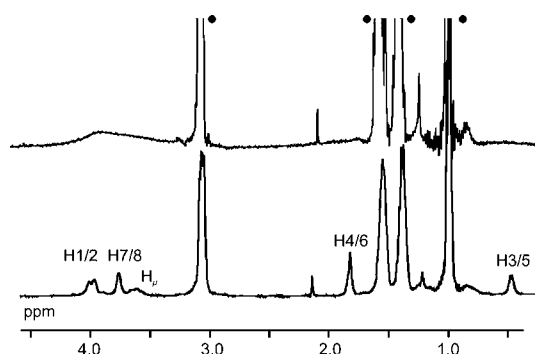

Figure 4. $^1H\{^{11}B\}$ NMR spectrum of $[N(n\text{-}Bu_4)][B_8H_9]$, measurement in CD_2Cl_2 at 27 °C (top) and -50 °C (bottom); ● = $[N(n\text{-}Bu_4)]^+$.

ature the $^1H\{^{11}B\}$ NMR spectrum shows a very broad signal (Figure 4). At -50 °C, five signals with an intensity of 2:2:1:2:2 were observed and assigned (H1/H2, δ 3.99 ppm; H7/H8, δ 3.76 ppm; H_μ, δ 3.61 ppm; H4/H6, δ 1.83 ppm; and H3/H5, δ 0.48 ppm; Figure 3). Our experimental work about the NMR behavior in solution confirms the theoretical studies of $[B_8H_8]^{2-}$ and $[B_8H_9]^-$.[17] It was possible to determine the coupling constant between H1/2 and H_μ ($^1J(^1H, ^1H) = 19$ Hz). Due to the fact that there are couplings between many protons, which are not well resolved, the bands are broad (calculated coupling constants can be found in the Supporting Information).

Crystal Structures of Salts of the $[B_8H_8]^{2-}$ and $[B_8H_9]^-$ Anions. The determination of the crystal structure of $[Zn(NH_3)_4]_2[B_8H_8]$ was published by Guggenberger in 1969.[39] This structure confirmed the D_{2d} dodecahedral geometry. The observed structure of $[B_8H_8]^{2-}$ is very similar to that found in B_8Cl_8,[41–43] $B_6H_6C_2(CH_3)_2$,[44] or $[CB_7H_8]^-$.[45] We have determined crystal structures of the dianion $[B_8H_8]^{2-}$ with various cations $[Cs^+$ and $[PPh_4]^+)$. For details, see Table 1 and the Supporting Information.

We were also able to crystallize $[PPh_4][B_8H_9]$ and $[N(n\text{-}Bu_4)][B_8H_9]$. The best structures were found for $[PPh_4]_2[B_8H_8]$ and $[PPh_4][B_8H_9]$. Both crystals were obtained by slow diffusion of diethyl ether into a solution of the respective compounds in dichloromethane. The crystallographic data are summarized in Table 2. A view of the monoanion $[B_8H_9]^-$ is shown in Figure 5.

A BHB bridge is formed upon protonation. $H\mu$ is found in the residual electron density as the strongest peak near B1 and
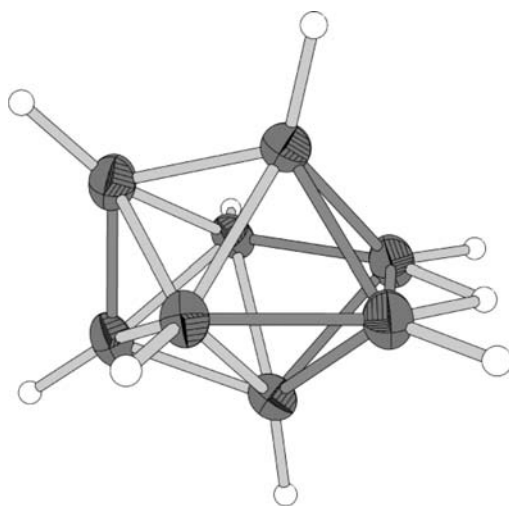
Figure 5. Structure of the $[B_8H_9]^-$ in $[PPh_4][B_8H_9]$ with 50% thermal ellipsoids for the B atoms (gray, shorter bonds as in $[B_8H_8]^{2-}$; dark gray, longer bonds as in $[B_8H_8]^{2-}$).

B2 and is located in one plane with B1, B2, B4, and B6. The refinement without H_μ leads to values for R, which are slightly worse than the refinement with H_μ ($R_1 = 0.0537/[I > 2\sigma(I)]$; 0.0603/all reflexes). The strongest peak (0.64 e$^-$/Å^3) in the

residual electron density was assigned to H_μ. This value is clearly higher than those of the other peaks (+0.42 e$^-$/Å^3 at P, deepest hole −0.47 at P). A peak for the alternative location for H_μ (B7−B8) was not found in the first 100 peaks (>0.1 e$^-$/Å^3, rms = 0.07 e$^-$/Å^3). The coordinates of H_μ were freely refined. The temperature factor was fixed to a value which is 1.5-times higher than U_{eq} (B1).

In comparison to the dianion, the monoanion shows a cluster deformation. The bonds, which are marked dark gray in Figure 5 (see also Table 3), are longer than those in $[B_8H_8]^{2-}$, while the other bonds are shorter. The biggest difference was found for the bond between B1 and B2 (0.051 Å), where the additional proton is located. All bonds, which are bonded to those two boron atoms B1 and B2, as well as the bond between B7 and B8, are elongated. In comparison to other protonated borates of the form $[B_nH_{n+1}]^-$ (n = 6, 7, 10), however, the boron−boron bonds in $[B_8H_9]^-$ show only small differences. In $[B_6H_7]^-$, where H_μ was located above one of the BBB faces, the difference of the bond length is about 0.14 Å.[7,8] H_μ was found in $[B_7H_8]^-$ mainly on an edge, but it also shows an interaction with a BBB face. The difference of this bond is about 0.19 Å.[10] Investigation of $[B_{10}H_{11}]^-$ established the fact that the proton caps one of the triangular faces. This results in a difference of the bond length of about 0.28 Å.[11] In summary, it can be said that the skeletal deformation in $[B_8H_9]^-$ compared to the

Table 1. Crystallographic Data for Cs$_2$[B$_8$H$_8$] (1) and [PPh$_4$]$_2$[B$_8$H$_8$]·CH$_2$Cl$_2$ (2, 3)

	1	2	3
temperature, K	150	150	100
space group	$Pnma$ (No. 62)	$P\bar{1}$ (No. 2)	$P\bar{1}$ (No. 2)
formula weight, g mol^{-1}	360.36	858.21	858.21
crystal size, mm	0.07·0.11·0.15	0.22·0.79·0.83	0.27·0.51·0.98
color	colorless	brown	brown
crystal system	orthorhombic	triclinic	triclinic
a, Å	11.0722(3)	11.1575(5)	11.11031(18)
b, Å	6.43096(19)	12.4392(5)	12.5143(2)
c, Å	13.7047(4)	18.6713(8)	18.6102(3)
α, deg	90	77.181(3)	76.9237(14)
β, deg	90	77.902(4)	77.1412(14)
γ, deg	90	69.363(4)	68.7870(16)
cell volume, Å^3	975.85(5)	2340.02(17)	2321.26(7)
Z	4	2	2
density (calcd), g cm^{-3}	2.453	1.218	1.228
absorption coefficient, mm^{-1}	7.386	0.241	0.243
F(000)	632	896	896
wavelength, Å	0.71073	0.71073	0.71073
measured θ area, deg	$3.50 \leq \theta \leq 32.70$	$3.09 \leq \theta \leq 29.50$	$3.10 \leq \theta \leq 32.89$
limiting indices	$-15 \leq h \leq 16$	$-13 \leq h \leq 14$	$-16 \leq h \leq 16$
	$-9 \leq k \leq 9$	$-15 \leq k \leq 15$	$-18 \leq k \leq 18$
	$-20 \leq l \leq 20$	$-25 \leq l \leq 24$	$-28 \leq l \leq 27$
completeness to θ/d	99.8%/30.5°/0.7 Å	99.7%/26.4°/0.8 Å	99.9%/30.5°/0.7 Å
reflexes: measured/independent/obsd $[I > 2\sigma(I)]$	11309/1821/1638	17081/10626/7833	51190/15639/13542
R(int)/$R(\sigma)$	0.0307/0.0209	0.0204/0.0431	0.0214/0.0212
data/parameters/restraints	1821/83/66	10626/557/0	15639/557/0
goodness-of-fit on F^2/restrained goodness-of-fit	1.095/1.084	1.043/1.043	1.056/1.056
R_1 obsd/all	0.0241/0.0295	0.0661/0.0921	0.0428/0.0509
wR_2	0.0549	0.1821	0.1150
largest diff peak and hole, e Å^{-3}	1.098/−0.948	0.601/−0.559	0.522/−0.328
a, b^a	0.0253/0.596	0.0753/2.1618	0.0550/1.0237
CCDC	838035	838036	838037

$^a w = 1/[\sigma^2(F_o^2) + (aP)^2 + bP]$, with $P = (\text{Max}(F_o^2, 0) + 2F_c^2)/3$.

Table 2. Crystallographic Data for $[Ph_4P][B_8H_9]$ (4, 5, 6) and $[N(n\text{-}Bu_4)][B_8H_9]$ (7)

	4	5	6	7[c]
temperature, K	100	150	293	100
space group	$P2/c$ (No. 13)	$P2/c$ (No. 13)	$P4/n$ (No. 85)	$P4_1$ (No. 76)/$P4_3$ (No. 78)
formula weight, g mol^{-1}	434.92	434.92	434.92	338.01
crystal size, mm	0.19·0.20·0.70	0.19·0.20·0.70	0.19·0.20·0.70	0.11·0.25·0.32
color	colorless	colorless	colorless	colorless
crystal system	monoclinic	monoclinic	tetragonal	tetragonal
a, Å	17.9396(5)	17.9817(4)	12.7049(4)	10.95583(15)
b, Å	7.6085(2)	7.6218(3)	12.7049	10.95583
c, Å	17.4663(4)	17.5188(4)	7.6363(3)	38.5800(10)
β, deg	92.169(2)	92.173(2)	90	90
cell volume, Å^3	2382.34(12)	2399.26(12)	1232.60(7)	4630.77(15)
Z	4	4	2	8
density (calcd), g cm^{-3}	1.213	1.204	1.172	0.970
absorption coefficient, mm^{-1}	1.073	1.065	1.037	0.341
$F(000)$	912	896	896	1504
wavelength, Å	1.54184	1.54184	1.54184	1.54184
measured θ area, deg	$4.93 \leq \theta \leq 62.55$	$4.92 \leq \theta \leq 62.55$	$4.92 \leq \theta \leq 60.83$	$4.04 \leq \theta \leq 61.01$
limiting indices	$-20 \leq h \leq 20$	$-20 \leq h \leq 20$	$-13 \leq h \leq 11$	$-9 \leq h \leq 11$
	$-8 \leq k \leq 6$	$-8 \leq k \leq 7$	$-12 \leq k \leq 14$	$-12 \leq k \leq 12$
	$-20 \leq l \leq 20$	$-20 \leq l \leq 19$	$-8 \leq l \leq 4$	$-43 \leq l \leq 43$
completeness to θ/d	99.7%/62.4°/0.87 Å	99.6%/62.4°/0.87 Å	99.3%/58.9°/0.9 Å	99.6%/58.9°/0.9 Å
reflexes: measured/independent/obsd $[I > 2\sigma(I)]$	34436/(3790)[a]/29932	28289/(3815)[b]/ 24086	1463/934/819	14044/6924/6192
R(int)/$R(\sigma)$	$-$[a]/0.0199	$-$[b]/0.0183	0.0122/0.0177	0.0293/0.0295
data/parameters/restraints	34436/298/0	28289/298/0	934/86/4	6924/657/573
goodness-of-fit on F^2/restrained goodness-of-fit	1.029/1.029	1.011/1.011	1.102/1.100	1.030/1.032
R_1 obsd/all	0.0525/0.0590	0.0720/0.0796	0.0439/0.0487	0.0851/0.0913
wR_2	0.1589	0.2200	0.1200	0.2397
extinction coefficient	0	0	0.0074(12)	0
largest diff peak and hole, e Å^{-3}	0.422/$-$0.467	0.593/$-$0.616	0.162/$-$0.421	0.444/$-$0.241
a, b[d]	0.1111/0.2569	0.1664/0.3471	0.0533/0.4119	0.1631/1.5400
CCDC	838038	838039	838040	838041

[a]Twin; for more details see the Supporting Information. [b]Twin; for more details see the Supporting Information. [c]Flack parameter $x = 0.35 \pm 0.70$. [d]$w = 1/[\sigma^2(F_o^2) + (aP)^2 + bP]$, with $P = (Max(F_o^2, 0) + 2F_c^2)/3$.

Table 3. Overview of the Bond Length in the $[PPh_4][B_8H_9]$ (4) and $[PPh_4]_2[B_8H_8]$ (3) Anions: Experimental and Calculated Values[17]

	$[PPh_4][B_8H_9]$ (4)		$[PPh_4]_2[B_8H_8]\cdot CH_2Cl_2$ (3)		
bond	exp (Å)	calcd[a] (Å)	exp (Å)	calcd[a] (Å)	Δ (d, Å)[d]
B_1–B_2	1.667(2)[b]	1.673 (1.686) [1.654]	1.616{4}	1.616	+0.051
B_1–$B_{3/5}$; B_2–$B_{3/5}$	1.851{2}[c]	1.852 (1.871) [1.833]	1.811{1}	1.822	+0.040
B_1–B_6; B_2–B_4	1.757{1}	1.768 (1.780) [1.770]	1.713{1}	1.709	+0.044
$B_{3/5}$–$B_{4/6}$	1.876{5}	1.882 (1.886) [1.867]	1.909{5}	1.909	$-$0.033
$B_{4/6}$–$B_{7/8}$	1.768{1}	1.764 (1.772) [1.752]	1.811{1}	1.822	$-$0.043
B_3–B_7; B_5–B_8	1.706{6}	1.703 (1.710) [1.703]	1.713{1}	1.709	$-$0.007
B_7–B_8	1.627(2)	1.627 (1.627) [1.627]	1.616{4}	1.616	+0.011

[a]Without parentheses, B3LYP/6-311++g(d,p) (this work); in parentheses, SCF/6-31G*; in brackets, MP2/6-31G*.[17] [b]Error of the measurement. [c]Statistical error (calculated with Origin 7G SR2 (v7.0394)). [d]Difference of the bond lengths of $[PPh_4][B_8H_9]$ and $[PPh_4]_2[B_8H_8]$.

$[B_8H_8]^{2-}$ dianion is smaller than the deformation of $[B_6H_7]^-$, $[B_7H_8]^-$, and $[B_{10}H_{11}]^-$ compared to $[B_6H_6]^{2-}$, $[B_7H_7]^{2-}$, and $[B_{10}H_{10}]^{2-}$, respectively. DFT calculations confirm that there are only small deformations in the B8 vertex upon protonation (see Table 3) and predict the bigger deformations of $[B_6H_7]^-$, $[B_7H_8]^-$, and $[B_{10}H_{11}]^-$.

Theoretical Aspects. In comparison to earlier studies, the presented calculations show some new aspects about $[B_8H_9]^-$.[17] It was possible to find a new transition state (No. 4), which was proved by hydrogen–deuterium exchange reactions. As mentioned before, the dynamic behavior of

$[B_8H_9]^-$ in solution is in agreement with the small activation energies for the minimum 0 (transition states 4 (41.3 kJ/mol) and 5 (51.2 kJ/mol), Table 4, Figure 6).

At room temperature all nine hydrogen atoms are dynamic in the ^{1}H NMR spectra (Figure 3). At -50 °C the nine hydrogen atoms show five signals with an intensity of 2:2:1:2:2. Only the transition state 4, which has not been reported before, allows the exchange of the terminal hydrogen atoms with H_μ. In this case, the migration of H_μ around the cluster scrambles all boron atoms. A section of the feasible rearrangements in $[B_8H_9]^-$ is summarized in Scheme 3.

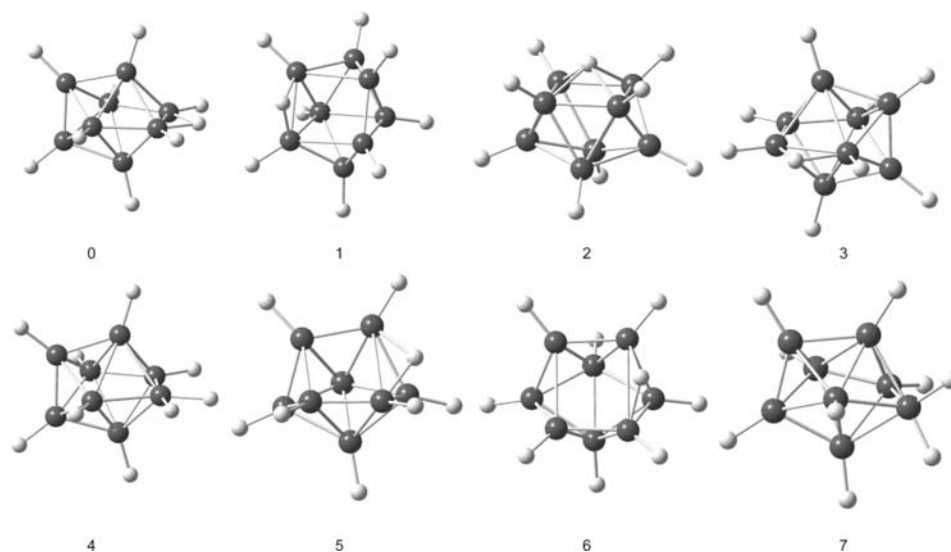**Figure 6.** Drawing of the minima (min.) and the transition states (TS) for $[B_8H_9]^-$.

Table 4. Minima and Transition States of $[B_8H_9]^-$

no.	no.[a]	P.G.	$\Delta E,^b$ kJ/ mol	$\Delta E_{(corr)},^b$ kJ/ mol	$\Delta E_{(corr)},^c$ kJ/ mol	comment
0	4a	C_{2v}	0	0	0	min.
1	4b	C_s	20.6	19.8	42.3	min.
2	4e	C_{2v}	36.7	26.3	45.6	TS
3	4d	C_s	37.8	34.8	53.6	TS
4		C_s	46.8	41.3	>209	TS
5	4c	C_s	55.4	51.2	77.4	TS
6	4f	C_s	99.7	91.3	132.6	TS
7		C_s	180.7	162.0	>209	TS

[a]Labeling in ref 17. [b]B3LYP/6-311++g(d,p) (this work). [c]MP2/6-31G* + ZPE(6-31G*).[17]

Scheme 3. Feasible Rearrangements in $[B_8H_9]^-$
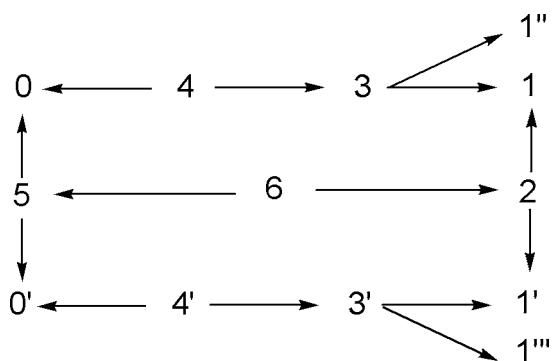
Supporting substitution experiments in aqueous medium were done (see Experimental Section). The substitution of H and D is in agreement with our calculations, and it was possible to prove the presence of the unknown transition state 4. In $[B_7H_7]^{2-}$, however, only the five equatorial protons were substituted under the same conditions.[10]

CONCLUSIONS

The monoanion $[B_8H_9]^-$ is easily prepared from $[B_8H_8]^{2-}$ in quantitative yield. The anion was characterized by NMR spectroscopy, and the dynamic behavior in solution was investigated. Experimental data are in agreement with calculated values. The structure of $[B_8H_9]^-$ was determined by single X-ray diffraction and compared to the other members of the series $M[B_nH_{n+1}]$ (M = 6, 7, and 10).

■ ASSOCIATED CONTENT

ⓢ Supporting Information

Calculated and experimental values for coupling constants and chemical shifts of $[B_8H_8]^{2-}$ and $[B_8H_9]^-$, and twin laws of crystal numbers 4 and 5. This material is available free of charge via the Internet at http://pubs.acs.org.

■ AUTHOR INFORMATION

Corresponding Author
*E-mail: edbern@uni-wuppertal.de.

■ ACKNOWLEDGMENTS

■ REFERENCES

(1) Hawthorne, M. F.; Pitochelli, A. R. *J. Am. Chem. Soc.* **1959**, *81*, 5519.
(2) Boone, J. L. *J. Am. Chem. Soc.* **1964**, *86*, 5036.
(3) Klanberg, F.; Eaton, D. R.; Guggenberger, L. J.; Muetterties, E. L. *Inorg. Chem.* **1967**, *6*, 1271.
(4) Klanberg, F.; Muetterties, E. L. *Inorg. Chem.* **1966**, *5*, 1955.
(5) Pitochelli, A. R.; Hawthorne, F. M. *J. Am. Chem. Soc.* **1960**, *82*, 3228.
(6) Kuznetsov, I. Y.; Vinitskii, D. M.; Solntsev, K. A.; Kuznetsov, N. T.; Butman, L. A. *Dokl. Akad. Nauk SSSR* **1985**, *283*, 873.
(7) Hofmann, K.; Prosenc, M. H.; Albert, B. R. *Chem. Commun. (Cambridge, U. K.)* **2007**, 3097.
(8) Förster, D.; Scheins, S.; Luger, P.; Lentz, D.; Preetz, W. *Eur. J. Inorg. Chem.* **2007**, 3169.
(9) Polyanskaya, T.; Drozdova, M.; Volkov, V.; Myakishev, K. *J. Struct. Chem.* **2009**, *50*, 368.
(10) Schlüter, F.; Bernhardt, E. *Inorg. Chem.* **2011**, *50*, 2580.
(11) Shore, S. G.; Hamilton, E. J. M.; Bridges, A. N.; Bausch, J.; Krause-Bauer, J. A.; Dou, D.; Liu, J.; Liu, S.; Du, B.; Hall, H.; Meyers, E. A.; Vermillion, K. E. *Inorg. Chem.* **2003**, *42*, 1175.
(12) Preetz, W.; Peters, G. *Eur. J. Inorg. Chem.* **1999**, 1831.
(13) Hawthorne, M. F.; Mavunkal, I. J.; Knobler, C. B. *J. Am. Chem. Soc.* **1992**, *114*, 4427.

(14) Wegner, P. A.; Adams, D. M.; Callabretta, F. J.; Spada, L. T.; Unger, R. G. *J. Am. Chem. Soc.* **1973**, *95*, 7513.

(15) Dewkett, W. J.; Grace, M.; Beall, H. *J. Inorg. Nucl. Chem.* **1971**, *33*, 1279.

(16) Bernhardt, E.; Brauer, D.; Finze, M.; Willner, H. *Angew. Chem.* **2007**, *119*, 2985; *Angew. Chem., Int. Ed.* **2007**, *46*, 2927.

(17) Buehl, M.; Mebel, A. M.; Charkin, O. P.; Schleyer, P. v. R. *Inorg. Chem.* **1992**, *31*, 3769.

(18) Kleier, D. A.; Lipscomb, W. N. *Inorg. Chem.* **1979**, *18*, 1312.

(19) Muetterties, E. L.; Wiersema, R. J.; Hawthorne, M. F. *J. Am. Chem. Soc.* **1973**, *95*, 7520.

(20) Muetterties, E. L. *Tetrahedron* **1974**, *30*, 1595.

(21) Muetterties, E. L.; Hoel, E. L.; Salentine, C. G.; Hawthone, M. F. *Inorg. Chem.* **1975**, *14*, 950.

(22) *CrysAlisPro*, version 1.171.33.42; Oxford Diffraction Ltd.: Oxford, U.K..

(23) Kohn, W.; Sham, L. J. *Phys. Rev. A* **1965**, *140*, 1133.

(24) Becke, A. D. *Phys Rev. B* **1988**, *38*, 3098.

(25) Lee, C.; Yang, W.; Parr, R. G. *Phys Rev. B* **1988**, *41*, 785.

(26) Becke, A. D. *J. Chem. Phys.* **1993**, *98*, 5648.

(27) Frisch, M. J.; Trucks, G. W.; Schlegel, H. B.; Scuseria, G. E.; Robb, M. A.; Cheeseman, J. R.; Montgomery, J. A., Jr.; Vreven, T.; Kudin, K. N.; Burant, J. C.; Millam, J. M.; Iyengar, S. S.; Tomasi, J.; Barone, V.; Mennucci, B.; Cossi, M.; Scalmani, G.; Rega, N.; Petersson, G. A.; Nakatsuji, H.; Hada, M.; Ehara, M.; Toyota, K.; Fukuda, R.; Hasegawa, J.; Ishida, M.; Nakajima, T.; Honda, Y.; Kitao, O.; Nakai, H.; Klene, M.; Li, X.; Knox, J. E.; Hratchian, H. P.; Cross, J. B.; Adamo, C.; Jaramillo, J.; Gomperts, R.; Stratmann, R. E.; Yazyev, O.; Austin, A. J.; Cammi, R.; Pomelli, C.; Ochterski, J. W.; Ayala, P. Y.; Morokuma, K.; Voth, G. A.; Salvador, P.; Dannenberg, J. J.; Zakrzewski, V. G.; Dapprich, S.; Daniels, A. D.; Strain, M. C.; Farkas, O.; Malick, D. K.; Rabuck, A. D.; Raghavachari, K.; Foresman, J. B.; Ortiz, J. V.; Cui, Q.; Baboul, A. G.; Clifford, S.; Cioslowski, J.; Stefanov, B. B.; Liu, G.; Liashenko, A.; Piskorz, P.; Komaromi, I.; Martin, R. L.; Fox, D. J.; Keith, T.; Al-Laham, M. A.; Peng, C. Y.; Nanayakkara, A.; Challacombe, M.; Gill, P. M. W.; Johnson, B.; Chen, W.; Wong, M. W.; Gonzalez, C.; Pople, J. A. *Gaussian 03*, Revision B.05; 2003.

(28) London, F. *J. Phys. Radium* **1937**, *8*, 397.

(29) McWeeny, R. *Phys. Rev.* **1962**, *126*, 1028.

(30) Ditchfield, R. *Mol. Phys.* **1974**, *27*, 789.

(31) Dodds, J. L.; McWeeny, R.; Sadlej, A. J. *Mol. Phys.* **1980**, *41*, 1419.

(32) Wolinski, K.; Hilton, J. F.; Pulay, P. *J. Am. Chem. Soc.* **1990**, *112*, 8251.

(33) Helgaker, T.; Watson, M.; Handy, N. C. *J. Chem. Phys.* **2000**, *113*, 9402.

(34) Sychrovsky, V.; Grafenstein, J.; Cremer, D. *J. Chem. Phys.* **2000**, *113*, 3530.

(35) Barone, V.; Peralta, J. E.; Contreras, R. H.; Snyder, J. P. *J. Phys. Chem. A* **2002**, *106*, 5607.

(36) Rienstra-Kiracofe, J. C.; Tschumper, G. S.; Schäfer, H. F.; Nandi, S.; Ellison, G. B. *Chem. Rev.* **2002**, *102*, 231.

(37) Gonzales, C.; Schlegel, H. B. *J. Chem. Phys.* **1989**, *90*, 2154.

(38) Gonzales, C.; Schlegel, H. B. *J. Phys. Chem.* **1990**, *94*, 5523.

(39) Guggenberger, L. J. *Inorg. Chem.* **1969**, *8*, 2771.

(40) Volkov, O.; Dirk, W.; Englert, U.; Paetzold, P. *Z. Anorg. Allg. Chem.* **1999**, *625*, 1193.

(41) Pawley, G. S. *Acta Crystallogr.* **1966**, *20*, 631.

(42) Jacobson, R. A.; Lipscomb, W. N. *J. Am. Chem. Soc.* **1958**, *80*, 5571.

(43) Jacobson, R. A.; Lipscomb, W. N. *J. Chem. Phys.* **1959**, *31*, 605.

(44) Hart, H. V.; Lipscomb, W. N. *Inorg. Chem.* **1968**, *7*, 1070.

(45) Jelínek, T.; Stíbr, B.; Pleek, J.; Kennedy, J. D.; Thornton-Pett, M. *J. Chem. Soc., Dalton Trans.* **1995**, 431.